Chemical Induction of Hsp70 Reduces α-Synuclein Aggregation in Neuroglioma Cells

Kiri Kilpatrick,[†] Jose Andres Novoa,[†] Tommy Hancock,[†] Christopher J. Guerriero,[‡] Peter Wipf,[§] Jeffrey L. Brodsky,[‡] and Laura Segatori*,[†,∥,⊥]

Departments of [†]Chemical and Biomolecular Engineering, [∥]Bioengineering, and [⊥]Biochemistry and Cell Biology, Rice University, Houston, Texas 77005, United States

Departments of [§]Chemistry and [‡]Biological Sciences, University of Pittsburgh, Pittsburgh, Pennsylvania 15260, United States

S *Supporting Information*

ABSTRACT: Misfolding and aggregation of α-synuclein (α-syn) is associated with the development of a number of neurodegenerative diseases including Parkinson's disease (PD). Analyses of *post mortem* tissues revealed the presence of molecular chaperones within α-syn aggregates, suggesting that chaperones play a role in α-syn misfolding and aggregation. In fact, inhibition of chaperone activity aggravates α-syn toxicity, and the overexpression of chaperones, particularly 70-kDa heat shock protein (Hsp70), protects against α-syn-induced toxicity. In this study, we investigated the effect of carbenoxolone (CBX), a glycyrrhizic acid derivative previously reported to upregulate Hsp70, in human neuroglioma cells overexpressing α-syn. We report that CBX treatment lowers α-syn aggregation and prevents α-syn-induced cytotoxicity. We demonstrate further that Hsp70 induction by CBX arises from activation of heat shock factor 1 (HSF1). The Hsp70 inhibitor MAL3-101 and the Hsp70 enhancer 115-7c led to an increase or decrease in α-syn aggregation, respectively, in agreement with these findings. In summary, this study provides a proof-of-principle demonstration that chemical modulation of the Hsp70 machine is a promising strategy to prevent α-syn aggregation.
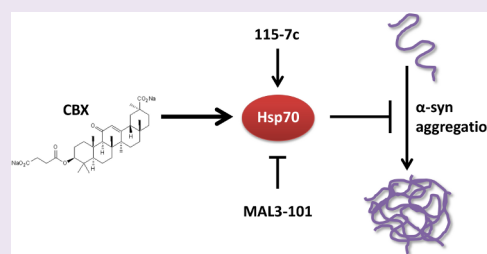
Protein misfolding and aggregation plays an important role in the progression of many human diseases. A number of neurodegenerative diseases are associated with the aggregation of α-synuclein (α-syn), a natively unfolded presynaptic protein with unknown function that has the propensity to misfold and aggregate.[1] Misfolded monomers tend to oligomerize into soluble protofibrillar structures and eventually aggregate in the form of insoluble deposits.[2] Accumulation of fibrillar α-syn is characteristic of a number of neurodegenerative diseases including Parkinson's disease (PD), dementia with Lewy bodies (DLB), pure autonomic failure (PAF), and multiple system atrophy (MSA), collectively referred to as synucleinopathies.[3]

Presently incurable and affecting 1 million people in the U.S. and more than 4 million people worldwide, PD is the most common neurodegenerative movement disorder. Substantial evidence links α-syn to both familial and sporadic PD. However, the molecular mechanisms underlying α-syn misfolding and the role of α-syn inclusions in the progression of PD pathogenesis remain elusive. Duplication and triplication of the α-syn locus and point mutations in the α-syn-encoding gene (A30P, E46K, and A53T) cause aberrant accumulation and aggregation of misfolded α-syn.[3,4] Overexpression of α-syn was also reported to induce aggregation and cytotoxicity in cell culture[5] and decreased motor performance and coordination in animal models.[6] Furthermore, overexpression of wild type and mutant α-syn in primary rat cell cultures caused increased sensitivity to neurotoxins and the death of dopaminergic neurons, respectively.[5]

Heat shock proteins (HSPs), ubiquitinated proteins, and components of the ubiquitin-proteasome system (UPS) accumulate within α-syn aggregates, implicating both protein misfolding and UPS dysfunction in PD and other synucleino-pathies.[7] The insoluble cytoplasmic aggregates that form upon overexpression of α-syn in cell culture colocalize with HSPs.[8] HSPs are highly conserved molecular chaperones that protect cells from proteotoxic stress by preventing protein misfolding and aggregation and by promoting the degradation of aberrantly accumulating misfolded proteins.[9] Particularly, the 70-kDa heat shock protein (Hsp70) was shown to interact with α-syn, to prevent α-syn aggregation, and to protect the cell from α-syn-induced toxicity.[10−12] Overexpression of Hsp70 was also reported to suppress the loss of dopaminergic neurons caused by α-syn accumulation in a *Drosophila* model[13] and to prevent α-syn aggregation in mice and in cell culture.[14] HSPs, such as Hsp70, are upregulated upon activation of Heat Shock Factor 1 (HSF1), which typically occurs as part of the cellular stress response to restore protein homeostasis.[15] Not surprisingly, HSF1 overexpression reduced α-syn accumulation and aggregation by enhancing Hsp70 expression.[16,17]

Based on these data, chemical modulation of Hsp70 provides a new avenue to prevent α-syn aggregation and, potentially, to treat protein misfolding diseases in which the formation of nonnative proteinaceous inclusion bodies is associated with neurodegeneration. To this end, a number of small molecules have been reported that upregulate Hsp70 expression with different mechanisms of action. For example, inhibition of proteasomal degradation using MG-132 and lactacystin induces HSF1 activation and HSP expression.[18] Celastrol, a quinone methide triterpene, induces HSF1 activation and Hsp70 upregulation with kinetics similar to heat shock.[19] Geranylgeranylacetone (GGA), a known antiulcer drug, was also reported to upregulate Hsp70 through activation of HSF1.[20] Hsp90 inhibitors, geldanamycin and 17-allylamino-17-demethoxygeldanamycin (17-AAG), were also shown to mediate Hsp70 upregulation and thus reduce α-syn aggregation.[21,22]

Carbenoxolone (CBX), a glycyrrhizic acid derivative, is widely used for the treatment of peptic ulcers[23] and was reported to have neuroprotective effects in animal models of isechemia.[24] Recent evidence showed that CBX activates HSF1 and upregulates Hsp70 levels in cells. However, it is unclear whether CBX treatment also leads to upregulation of other HSPs.[25−27] In addition, the molecular mechanism involved in the activation of HSF1 induced by CBX treatment is elusive. Evidence suggests that CBX induces membrane potential collapse and ROS generation by interacting with the respiratory chain in the mitochondria, thereby causing oxidative stress.[28] It was therefore hypothesized that the heat shock response is activated as part of the cellular response to CBX-induced oxidative stress.

In this study, we investigated whether treatment with CBX prevents α-syn aggregation in human neuroglioma cells. We generated a human neuroglioma cell line stably transfected for the overexpression of α-syn fused to GFP to facilitate visualization of the soluble and aggregated protein. We then demonstrated that treatment with CBX lowers α-syn aggregation. Mechanistic studies revealed that CBX treatment activates HSF1 and thereby upregulates Hsp70. The mechanism of CBX-mediated upregulation of Hsp70 involves mild induction of oxidative stress. However, CBX treatment did not result in cytotoxicity or apoptosis induction under conditions that prevented α-syn aggregation. Additionally, we report that direct chemical modulation of Hsp70 activity dramatically affects α-syn aggregation, confirming the role of the Hsp70 machine as a potential therapeutic target for the treatment of synucleinopathies and perhaps other neurodegenerative diseases associated with protein aggregation.

■ RESULTS AND DISCUSSION

CBX Treatment Prevents α-syn Aggregation. In order to evaluate whether treatment with CBX influences the formation of α-syn aggregates, we treated H4 cells stably transfected for the expression of α-syn fused to GFP at its C-terminal end (H4/α-syn-GFP) and evaluated the relative amount of α-syn-GFP that accumulates in insoluble aggregates. The use of α-syn-GFP as a valid reporter for disease-associated phenotypes has been previously established.[29,30] We investigated α-syn aggregation in H4/α-syn-GFP cells incubated with a range of CBX concentrations for 16 h by monitoring GFP fluorescence and binding of the ProteoStat dye, a 488-nm excitable red fluorescent molecule that specifically interacts with denatured proteins within protein aggregates.[31] Cells treated with MG-132 (0.5 μM), a proteasome inhibitor previously

reported to induce protein aggregation in cell cultures[31] were used as positive control. Fluorescent images (Figure 1a, columns 1 and 2) were merged and quantified using the ImageJ script *Colocalization Colormap* (see Methods) to
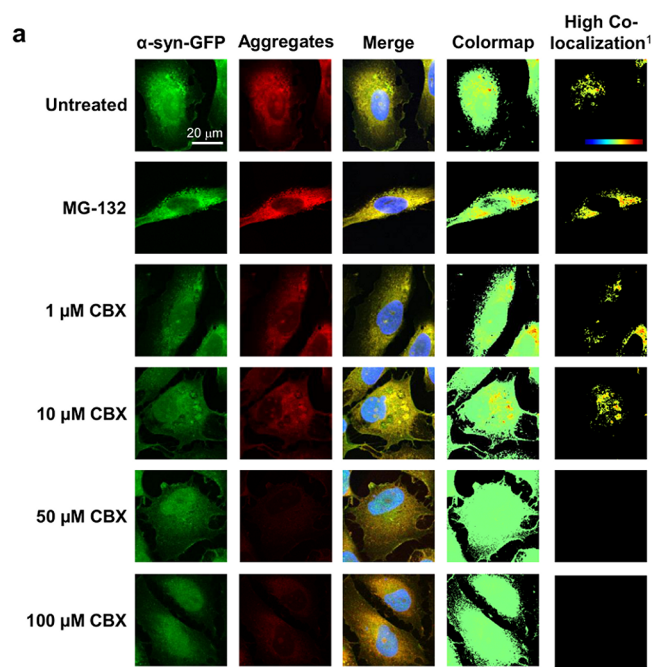
¹ Images filtered using color threshold to display positive correlation (Hue range 1-60).
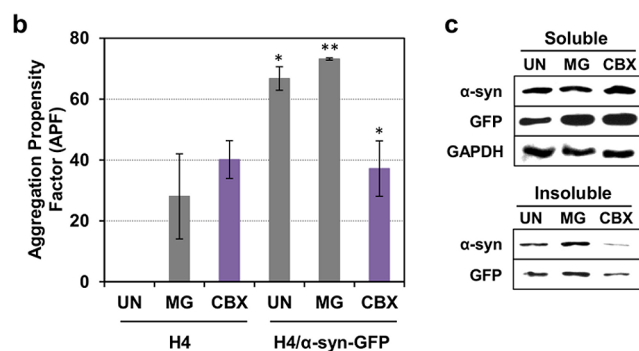
Figure 1. CBX decreases α-syn-containing aggregates and reduces total protein aggregation in H4/α-syn-GFP cells. (a) H4/α-syn-GFP cells untreated or treated with MG-132 (0.5 μM) or CBX (1, 10, 50, or 100 μM) for 16 h were analyzed by fluorescence microscopy. Images of α-syn-GFP fluorescence (green, column 1) and aggregates, detected using the ProteoStat dye (red, column 2), were merged (column 3) and analyzed using NIH ImageJ software. Colocalization of α-syn-GFP and ProteoStat dye were evaluated using the *Colocalization Colormap* plugin (column 4): "hot" colors represent a positive correlation and "cold" colors represent a negative correlation. High colocalization represented by hot colors was depicted by filtering colormap images based on hue as described in Methods (pixels 1−60) (column 5). Scale bar represents 20 μm. (b) Total protein aggregation in H4 and H4/α-syn-GFP cells untreated or treated with MG-132 (0.5 μM) or CBX (50 μM) for 16 h (*p < 0.05, **p < 0.005). Total protein aggregation was quantified by measuring binding of the ProteoStat dye by flow cytometry. The aggregation propensity factor (APF) was calculated as described in Methods. The data are reported as the mean ± SD (n = 3). (c) Western blot analyses of Triton X-100 soluble and insoluble α-syn and GFP in H4/α-syn-GFP cells treated with MG-132 (0.5 μM) or CBX (50 μM) for 16 h. GAPDH was used as a loading control.

evaluate the extent of colocalization of α-syn-GFP and the ProteoStat dye, which provides a read-out for α-syn-GFP aggregation. Detection of α-syn aggregation in H4/α-syn-GFP cells in the presence or absence of MG-132 was demonstrated by the punctate GFP fluorescence (column 1) and by the hot colors in the filtered colocalization colormaps (high colocalization, column 5). However, α-syn-GFP aggregation decreased in H4/α-syn-GFP cells treated with CBX in a concentration-dependent manner. Specifically, α-syn-GFP aggregation was undetectable in H4/α-syn-GFP cells treated with a concentration of CBX greater than 50 μM, as shown by the lack of colocalization between α-syn-GFP and the aggregation-specific dye (Figure 1a, rows 5 and 6). Additional images are displayed in the Supporting Information (Supplementary Figure S1).

α-syn-GFP aggregation was also evaluated by quantifying the extent of colocalization between the dye and α-syn-GFP in single cells (Table 1). MG-132 treatment resulted in an

Table 1. Quantitative Analysis of α-syn Aggregation in H4/α-syn-GFP Cells Treated with CBX (ProteoStat−α-syn-GFP Colocalization)

cell treatment	high colocalization[a]	low colocalization[a]
untreated	59.7 ± 14.1	92.8 ± 11.0
MG-132	72.2 ± 29.4	83.3 ± 33.3
CBX*	5.6 ± 9.6	43.5 ± 12.3

[a]The degree of colocalization was determined by filtering colormap images based on hue: high colocalization was defined as pixels 1−35, and low colocalization was defined as pixels 35−60 (*$p < 0.05$). The percentage of cells that contained high and low colocalization was calculated by analyzing multiple images obtained from independent experiments and averaged over three experiments. The data are reported as the mean ± SD.

increase in the percentage of cells containing high colocalization (72.2%) compared to untreated H4/α-syn-GFP cells (high: 59.7%; low: 92.8%), as expected.[31] Treatment with CBX caused a dramatic decrease in the percentage of cells displaying high (5.6%) and low (43.5%) colocalization compared to untreated H4/α-syn-GFP cells.

Next, we compared the effect that CBX treatment has on protein aggregation in H4/α-syn-GFP cells and in H4 cells that lacked the α-syn-GFP overexpression vector. This experiment was conducted to measure how this treatment might generally impact cellular protein homeostasis, since a significant percentage of all proteins are aggregation-prone.[32] H4 and H4/α-syn-GFP cells were treated and imaged as described above, and the average pixel intensity of the ProteoStat dye was calculated to quantify total protein aggregation. Treatment of H4/α-syn-GFP cells with CBX (50 μM) caused a 2.3-fold decrease in cellular aggregation compared to untreated cells (Supplementary Table S1), consistent with the data in Table 1. The average intensity of the aggregation-specific dye detected in H4 cells in the presence or absence of MG-132 (0.5 μM) was similar to that observed in H4/α-syn-GFP cells under the same conditions. Interestingly, while CBX treatment again decreased aggregation in H4/α-syn-GFP cells (2.3-fold), it caused a mild increase in general protein aggregation in H4 cells (1.6-fold) compared to untreated cells. These results suggest that administration of CBX to otherwise healthy cells can promote some degree of cellular protein aggregation, perhaps due to the action of CBX inhibition on connexins, and subsequently, cell cycle control.[33] In contrast, CBX treatment of cells

accumulating aberrant misfolded and aggregation-prone proteins (H4/α-syn-GFP cells) exhibits a protective effect.

To quantify the effects of small molecule treatment on the extent of total protein aggregation, we calculated the aggregation propensity factor (APF; see Methods) of H4 and H4/α-syn-GFP cells treated with MG-132 (0.5 μM) and CBX (50 μM) relative to untreated H4 cells. The fluorescence of ProteoStat dye relative to untreated H4 cells was measured by flow cytometry (Figure 1b). We found that the APF of H4 cells was enhanced to 28.1% upon incubation with MG-132 and to 30.6% upon incubation with CBX. Untreated H4/α-syn-GFP cells displayed an APF of 67.0%, and MG-132 treatment increased the APF to 73.2%. However, CBX treatment caused a dramatic decrease in aggregate dye binding, thus lowering the APF of H4/α-syn-GFP cells to 37.2%. These findings confirm the results obtained with fluorescence microscopy.

α-syn-GFP aggregation in H4/α-syn-GFP cells treated with MG-132 (0.5 μM) or CBX (50 μM) was also confirmed by evaluating the relative accumulation of α-syn in Triton X-100 soluble and insoluble protein fractions by Western blot. Accumulation of soluble α-syn was largely unchanged upon MG-132 treatment but was considerably enhanced by CBX treatment. Consistent with this result, CBX also decreased the amount of insoluble α-syn compared to the untreated control (Figure 1c). These results are in agreement with what was observed from the florescence microscopy and flow cytometry studies above, and confirm that CBX treatment reduces α-syn aggregation. CBX treatment did not alter α-syn transcription, as evaluated by quantitative RT-PCR (Supplementary Figure S2), suggesting that CBX mediated reduction in α-syn aggregation is not due to an effect on α-syn expression. Interestingly, α-syn accumulation in the insoluble fraction increased upon treatment with MG-132, in agreement with the data in Figure 1b. The apparent net increase in the amount of α-syn-GFP in MG-132-treated cells (i.e., soluble and insoluble fractions) is consistent with a fraction of this protein being targeted for proteasome-mediated degradation.[7]

CBX Upregulates Hsp70 in H4/α-syn-GFP Cells. CBX was previously reported to induce the expression of HSPs, particularly Hsp70, by activating HSF1.[26] Thus, we asked whether CBX treatment prevents α-syn aggregation by upregulating Hsp70. We demonstrate here that Hsp70 mediates a reduction of α-syn aggregation in H4/α-syn-GFP cells treated with CBX using five independent experiments designed to evaluate Hsp70 expression (Figure 2), the effect of Hsp70 activity on α-syn aggregation and solubility (Figures 3 and 4), and activation of HSF1 (Figure 5).

The relative mRNA expression levels of Hsp70 (NM_005345) in H4 and H4/α-syn-GFP cells treated with CBX (50 μM) were evaluated by quantitative RT-PCR as previously described[34] and compared to the expression levels of Hsp27 (X54079), Hdj1 (Hsp40 (NM_006145)), and Hsp90 (NM_005348). As anticipated, we observed that Hsp70 expression was upregulated upon CBX treatment in H4 (2.1-fold) and H4/α-syn-GFP (3.0-fold) cells. We found that CBX treatment did not considerably alter the mRNA expression levels of Hsp27, Hdj1, or Hsp90 in H4 cells and resulted in a modest increase in the mRNA expression levels of Hsp27 (1.7-fold) and Hsp90 (1.9-fold) but not Hsp40 in H4/α-syn-GFP cells (Figure 2a). Interestingly, Hsp27, which was previously reported to modulate α-syn-induced toxicity in cell culture,[35] was not found to be considerably upregulated by CBX, suggesting that CBX-mediated reduction of α-syn aggregation
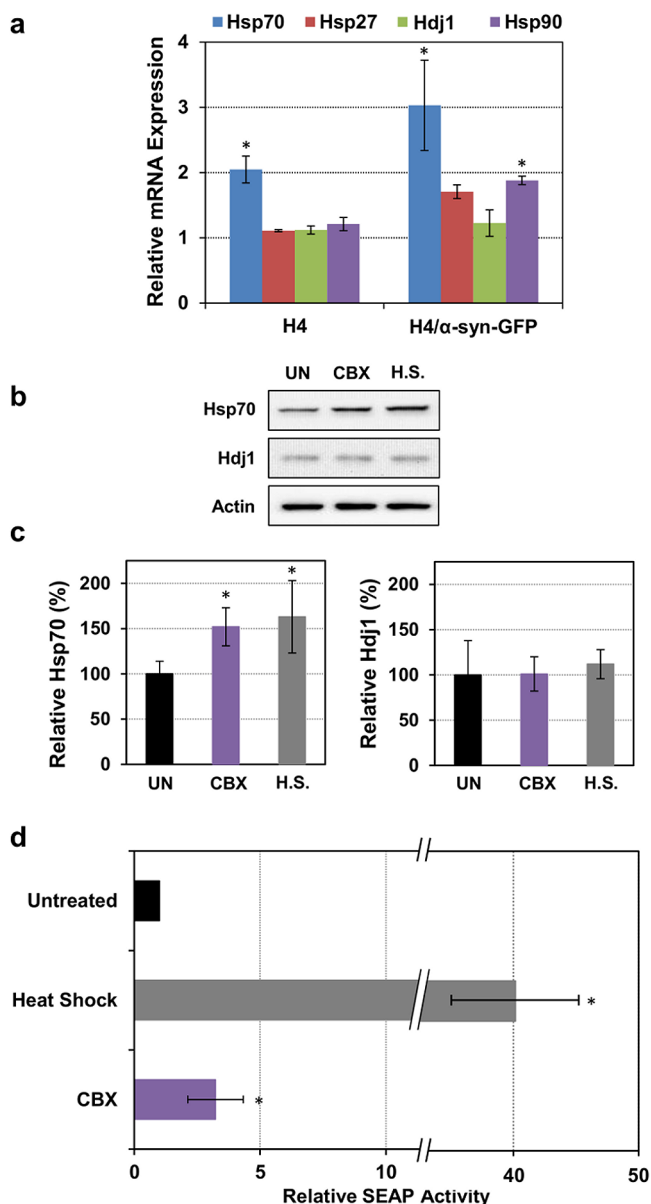
Figure 2. CBX induces Hsp70 expression in H4/α-syn-GFP cells. (a) Relative mRNA expression of Hsp70, Hsp27, Hdj1, and Hsp90 in H4 and H4/α-syn-GFP cells was measured after treatment with CBX (50 μM) for 16 h (*$p < 0.05$). mRNA expression levels were evaluated by quantitative RT-PCR, corrected for the expression of the housekeeping gene, GAPDH, and normalized to those of untreated cells. The data are reported as the mean $\pm$ SD ($n = 3$). (b) Western blot analyses of Hsp70 in H4/α-syn-GFP cells subjected to heat shock or treated with CBX (50 μM) for 16 h. Actin expression was used as a loading control. (c) Quantification of Hsp70 bands detected by Western blot in CBX-treated samples (*$p < 0.05$). Band analyses and quantifications were conducted using NIH ImageJ software. Experiments were repeated three times, and data points are reported as mean $\pm$ SD. (d) SEAP reporter assay using an expression vector that contains the promoter region of human Hsp70 gene fused to the gene encoding secreted embryonic alkaline phosphatase in H4/α-syn-GFP cells untreated or subjected to heat shock or treated with CBX (50 μM) (*$p < 0.05$). SEAP activity was evaluated by measuring the absorbance of QUANTI-Blue reagent and normalized to untreated H4/α-syn-GFP cells. The data are reported as the mean $\pm$ SD ($n = 3$).

does not depend on Hsp27. These results are also consistent with previous studies suggesting that CBX-induced expression

of HSPs varies depending on cell type and on the concentration of CBX used.[25,26] The increase in Hsp70 expression upon CBX treatment observed at the transcriptional level was confirmed at the protein level by evaluating the accumulation of Hsp70 by Western blot (Figure 2b). Treatment of H4/α-syn-GFP cells with CBX results in a 52% increase in Hsp70 protein (Figure 2c), which is comparable to what was observed in cells subjected to heat shock. However, treatment of H4/α-syn-GFP cells with CBX was found not to affect the accumulation of Hdj1, an Hsp40 cochaperone, which regulates the formation of complexes between Hsp70 and client proteins, and is thus expected to affect Hsp70-mediated folding (Figure 2b,c).[9] These data suggest that, among HSPs, Hsp70 is the primary and perhaps only mediator of the CBX effect on α-syn-GFP aggregation.

The effect of CBX on Hsp70 expression was also confirmed by monitoring the activation of the Hsp70 promoter in H4/α-syn-GFP cells treated with CBX. H4/α-syn-GFP cells were transfected with pDRIVE5SEAP-hHSP70 (Invivogen), a vector engineered for the expression of embryonic alkaline phosphatase (SEAP) under the control of human Hsp70 promoter, and were then treated with CBX (100 μM) for 8 h. CBX treatment resulted in a 3.2-fold increase in SEAP expression compared to untreated H4/α-syn-GFP cells (Figure 2d, also see Supplementary Figure S3). Activation of the Hsp70 promoter induced by heat shock (40-fold increase) is reported here for comparison. These results suggest that moderate upregulation of Hsp70 is sufficient to reduce α-syn-GFP aggregation.

To evaluate whether the decrease in α-syn aggregation observed in H4/α-syn-GFP cells treated with CBX depends on Hsp70 activity, we monitored aggregate dye binding upon inhibition of Hsp70 activity using MAL3-101, a compound that blocks the interaction between Hsp40 cochaperones and Hsp70 and inhibits the stimulation of ATP hydrolysis in vitro.[36] MAL3-101 was previously shown to inhibit Hsp70 activity in cells and in cell culture systems.[37−40] α-syn-GFP aggregation was examined by evaluating GFP and ProteoStat dye fluorescence in H4/α-syn-GFP cells treated with CBX (50 μM) and/or MAL3-101 (10 μM). We found that MAL3-101 inhibited the ability of CBX to prevent α-syn-GFP aggregation (Figure 3a, compare CBX to CBX+MAL3-101 images). Also, as might be anticipated, MAL3-101 on its own failed to solubilize α-syn-GFP, consistent with the requirement for Hsp70 to mediate this activity.

To quantify the effect of MAL3-101 treatment on CBX-mediated reduction in α-syn aggregation, we monitored ProteoStat dye binding by flow cytometry in H4/α-syn-GFP cells treated with CBX and MAL3-101 and calculated the aggregation propensity factor (APF; see Methods) of cells treated with CBX and MAL3-101 relative to untreated cells. CBX treatment resulted in dramatic decrease in ProteoStat dye binding (APF = −17%; Figure 3b). As expected, MAL3-101 treatment was found to increase ProteoStat dye binding (APF = 6.3%) compared to untreated cells. We also observed an increase in ProteoStat dye binding upon addition of MAL3-101 to CBX-treated cells (APF = 9.7%). These data are in agreement with the results obtained from the fluorescence microscopy analysis (Figure 3a) and suggest that MAL3-101 prevents CBX-induced reduction in α-syn aggregation in H4/α-syn-GFP cells. Together, these results confirm that CBX-induced Hsp70 upregulation plays a key role in preventing α-syn-GFP aggregation and that inhibition of Hsp70 by MAL3-

a

| | α-syn-GFP | Aggregates | Merge | Colormap | High Co-localization[1] |

Untreated, CBX, MAL3-101, CBX + MAL3-101

[1] Images filtered using color threshold to display positive correlation represented by hot colors (hue range 1-60).
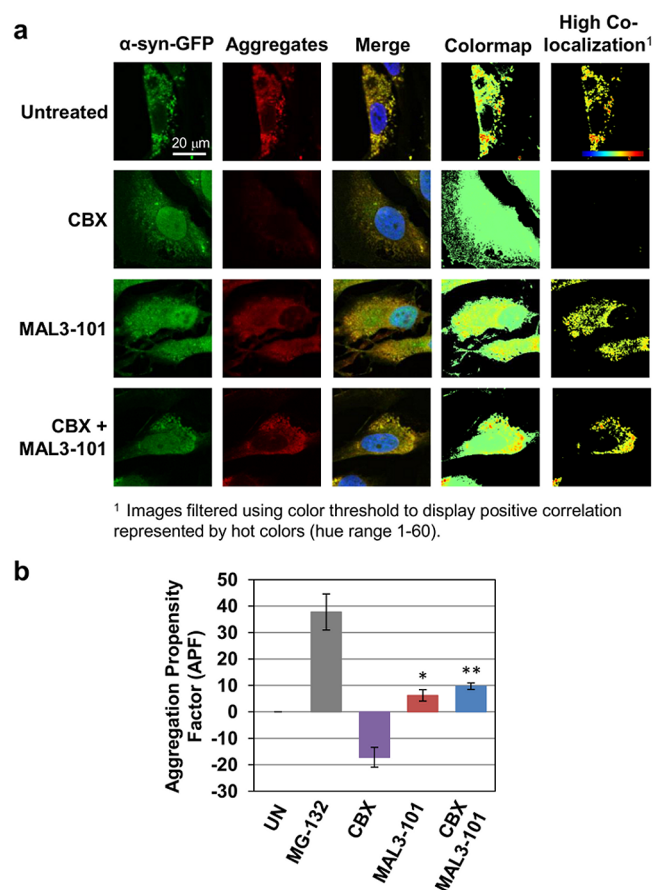
b

Figure 3. Inhibition of Hsp70 causes α-syn aggregation in H4/α-syn-GFP cells treated with CBX. (a) Fluorescence microscopy of H4/α-syn-GFP cells untreated or treated with CBX (50 μM) and/or MAL3-101 (10 μM) for 16 h. Images were analyzed as described in Figure 1. Scale bar represents 20 μm. (b) Total protein aggregation in H4/α-syn-GFP cells untreated or treated with CBX (50 μM) and/or MAL3-101 (10 μM) for 16 h. Total protein aggregation was quantified by measuring binding of the ProteoStat aggregation dye by flow cytometry. The APF was calculated as described in Figure 2. The data are reported as the mean ± SD (n = 3).

101 promotes the formation of α-syn-GFP into insoluble aggregates.

To further explore the effect of chemical modulation of Hsp70 activity on α-syn aggregation, we examined aggregate dye binding upon enhancement of Hsp70 activity. Hsp70 was activated by treating H4/α-syn-GFP cells with 115-7c (UPCMLD00WMAL1−271; PubChem CID 5461551), a small molecule that binds to a region of Hsp70 adjacent to the surface involved in J-domain stimulation and that works in cooperation with Hsp40 cochaperones to enhance nucleotide hydrolysis *in vitro*.[41,42] The specificity of 115-7c binding to Hsp70 was previously demonstrated, validating the use of this compound to investigate Hsp70 activity.[42] α-syn-GFP aggregation was tested by monitoring GFP and ProteoStat dye fluorescence in H4/α-syn-GFP cells treated with a range of 115-7c concentrations for 16 h. Treatment with 115-7c lowered α-syn aggregation at all concentrations tested as shown by the loss of colocalization between α-syn-GFP and the ProteoStat dye compared to untreated cells (Figure 4a). We also investigated the effect of Hsp70 activation in H4/α-syn-GFP cells treated with CBX. To quantify the effects of 115-7c treatment on CBX-induced decrease of total protein
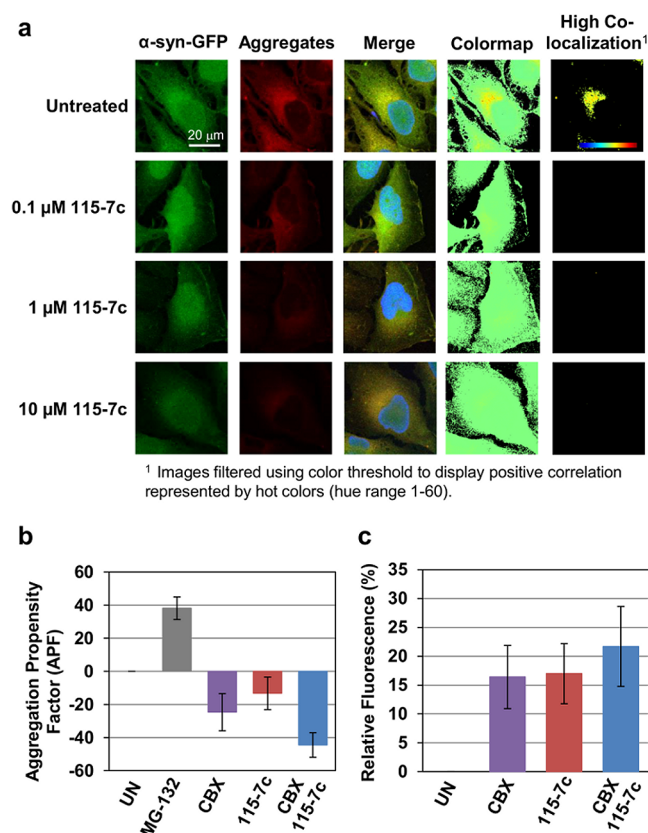
a

| | α-syn-GFP | Aggregates | Merge | Colormap | High Co-localization[1] |

Untreated, 0.1 μM 115-7c, 1 μM 115-7c, 10 μM 115-7c

[1] Images filtered using color threshold to display positive correlation represented by hot colors (hue range 1-60).

b

c

Figure 4. Activation of Hsp70 reduces α-syn aggregation in H4/α-syn-GFP cells treated with CBX. (a) Fluorescence microscopy of H4/α-syn-GFP cells untreated or treated with 115-7c (0.1, 1, and 10 μM) for 16 h. Images were analyzed as described in Figure 1. Scale bar represents 20 μm. (b) Total protein aggregation in H4/α-syn-GFP cells untreated or treated with CBX (50 μM) and/or 115-7c (1 μM) for 16 h. Total protein aggregation was quantified by measuring binding of the ProteoStat aggregation dye by flow cytometry. The APF was calculated as described in Figure 2. The data are reported as the mean ± SD (n = 3). (c) H4 cells were transfected to express the α-syn-split GFP system and treated with CBX (50 μM) and/or 115-7c (1 μM) for 16 h. Fluorescence complementation was evaluated by measuring GFP fluorescence by flow cytometry. Relative fluorescence was calculated by normalizing the fluorescence of treated cells to that of untreated cells. The data are reported as the mean ± SD (n = 3).

aggregation, we monitored ProteoStat dye binding by flow cytometry in H4/α-syn-GFP cells treated with CBX and 115-7c and calculated the aggregation propensity factor (APF; see Methods) relative to that of untreated cells. 115-7c treatment decreased ProteoStat dye binding (APF = −13.2%) compared to untreated cells, and cotreatment with 115-7c and CBX further reduced ProteoStat dye binding (APF = −44.4%) (Figure 4b). These results confirm the role of Hsp70 in preventing α-syn aggregation and suggest that chemical upregulation of Hsp70 expression and activity both affect α-syn aggregation.

To further confirm that chemical modulation of Hsp70 expression and activity prevents accumulation of α-syn aggregates by increasing α-syn solubility, we used an α-syn-split GFP complementation assay. In this assay, GFP is cleaved into two unequal size fragments: a large "detector" fragment (GFP$_{1−10}$) and a short β-sheet "sensor" fragment (GFP$_{11}$), which when fused to a protein of interest functions as a sensor of protein solubility.[43] In this assay, the sensor fragment was

fused to α-syn. Fluorescence complementation occurs only when α-syn is maintained in soluble form and the sensor fragment is accessible to the detector fragment. As a result, GFP fluorescence is a measurement of α-syn solubility and is inversely proportional to α-syn aggregation.[44] A transfection control consisting of a plasmid encoding a red fluorescent protein (mCherry) was included to account for differences in expression levels of α-synGFP$_{11}$ or GFP$_{1-10}$, as previously described.[44] The effect of Hsp70 on α-syn-GFP solubility was evaluated by monitoring GFP fluorescence in H4 cells expressing α-syn-GFP$_{11}$ and GFP$_{1-10}$ and treated with CBX and 115-7c. GFP fluorescence increased in cells treated with CBX (16.4%) and 115-7c (17.0%) and cotreated with CBX and 115-7c (21.7%) (Figure 4c). These results confirm that Hsp70 prevents α-syn aggregation by enhancing its solubility.

CBX Reduces α-syn Aggregation by Activating HSF1. Hsp70 and other heat shock proteins are upregulated upon HSF1 activation. In mammalian cells, HSF1 activation is a multistep process that involves the phosphorylation and translocation of HSF1 from the cytoplasm to the nucleus and the formation of large, irregularly shaped HSF1 granules.[15] HSF1 granules were previously observed in the nuclei of CBX-treated cells, suggesting that CBX causes HSP upregulation by activating HSF1.[26] Therefore, we evaluated the intracellular localization of HSF1 in H4/α-syn-GFP cells treated with CBX. Cells were incubated with the Hoechst 33342 fluorescent stain that allows visualization of the nuclei (Figure 5a, row 1) and with a fluorescently labeled anti-HSF1 antibody (Figure 5a, row 2), and images were analyzed as described above. Under control conditions, HSF1 resided throughout the nucleus in untreated H4/α-syn-GFP cells. Upon heat shock (42 °C for 2 h), HSF1-positive granules formed in the nuclei (arrows in Figure 5a) are characteristic of HSF1 activation.[45] Treatment of H4/α-syn-GFP cells with CBX for 2 and 4 h resulted in the formation of HSF1 granules similar to those observed upon heat shock, consistent with the notion that the effect of CBX is mediated through HSF1 activation.

To demonstrate that Hsp70 induction by CBX and the consequent reduction in α-syn aggregation is HSF1-dependent, H4/α-syn-GFP cells were treated with KNK-437, a known inhibitor of the heat shock response.[46] α-syn-GFP aggregation was examined by evaluating GFP and ProteoStat dye fluorescence in H4/α-syn-GFP cells treated with CBX (50 μM) and KNK-437 (10 μM). KNK-437 treatment was verified to promote protein aggregation in H4 cells (Supplementary Figure S4a) and resulted in a decrease in α-syn solubility as verified using the α-syn-split GFP complementation (Supplementary Figure S4b). As expected, KNK-437 failed to solubilize α-syn-GFP (Figure 5b). Co-treatment with KNK-437 and CBX resulted in an increase in α-syn-GFP aggregation compared to treatment with CBX, suggesting that KNK-437 treatment counteracts the effect of CBX (Figure 5b, compare CBX to CBX+KNK-437 images). To quantify the effects of KNK-437 treatment on CBX-mediated reduction of α-syn aggregation, we monitored ProteoStat dye binding by flow cytometry in H4/α-syn-GFP cells treated with CBX and 115-7c and calculated the aggregation propensity factor (APF; see Methods) relative to untreated cells. KNK-437 treatment increased ProteoStat dye binding (APF = 12.8%) compared to untreated cells. While CBX treatment, as reported above, lowers the ProteoStat dye binding (APF = −17%), the addition of KNK-437 to cells treated with CBX resulted in an increase in ProteoStat dye binding (APF = 11.9%) (Figure 5c). Together, these results
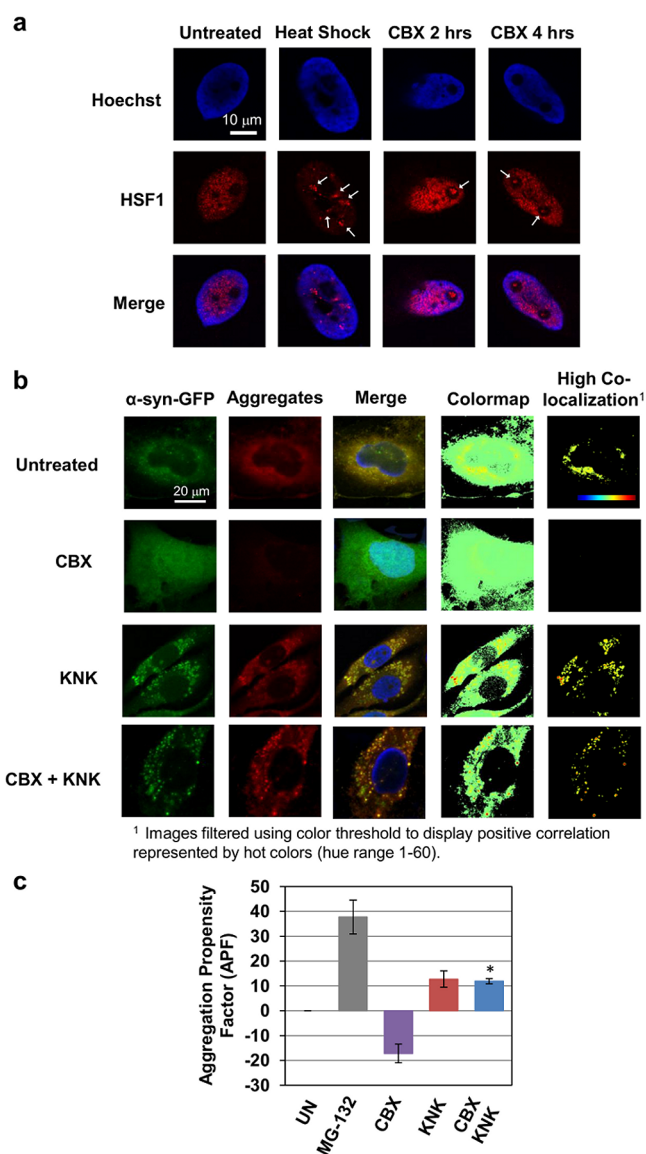

Figure 5. HSF1 is activated in H4/α-syn-GFP cells treated with CBX. (a) H4/α-syn-GFP cells untreated or subjected to heat shock (42 °C for 2 h followed by 4 h incubation at 37 °C) or treated with CBX (50 μM for 2 or 4 h) were analyzed by immunofluorescence microscopy to monitor HSF1 localization. The nucleus was detected with Hoechst 33342 fluorescent stain (blue, column 1), and HSF1 was detected using a rabbit anti-HSF1 antibody (red, column 2). Arrows indicate HSF1-positive stress granules. Images were analyzed and merged (column 3) using NIH ImageJ software. Scale bar represents 10 μm. (b) Fluorescence microscopy of H4/α-syn-GFP cells untreated or treated with CBX (50 μM) and/or KNK-437 (10 μM) for 16 h. Images were analyzed as described in Figure 1. Scale bar represents 20 μm. (c) Total protein aggregation in H4/α-syn-GFP cells untreated or treated with CBX (50 μM) and/or KNK-437 (10 μM) for 16 h. Total protein aggregation was quantified by measuring binding of the ProteoStat aggregation dye by flow cytometry. The APF was calculated as described in Figure 2. The data are reported as the mean ± SD ($n = 3$).

confirm that CBX-induced Hsp70 upregulation is HSF1-dependent and that inhibition of the heat shock response by KNK-437 promotes α-syn aggregation.

CBX Induces Moderate Oxidative Stress. CBX induces the collapse of mitochondria membrane potential and production of reactive oxygen species (ROS) in neurons.[28,47]

Oxidative stress has been repeatedly observed to induce Hsp70 upregulation via HSF1 activation, which in turn lowers proteotoxicity caused by ROS damage and protein misfolding.[15,48,49] Hence, it was speculated that the cytoprotective effect of CBX is mediated through induction of oxidative stress. We asked whether CBX treatment induces oxidative stress in H4/α-syn-GFP cells. Oxidative stress was evaluated using dihydrorhodamine 6G, a cell-permeable molecule that is oxidized to fluorescent rhodamine 6G upon induction of oxidative stress.[50] H4 and H4/α-syn-GFP cells were treated with MG-132 (0.5 μM) or CBX (50 μM) for 16 h, and rhodamine 6G (R6G) fluorescence was measured by flow cytometry. H_2O_2 treatment, under conditions previously reported to cause oxidative stress (100 μM for 1 h),[51] was used as a positive control in this experiment (Supplementary Figure S5). H_2O_2 and MG-132 resulted in 39.4% and 34.6% increases in R6G fluorescence, respectively, in H4/α-syn-GFP cells (Figure 6a). Treatment with CBX resulted in an 11.7%
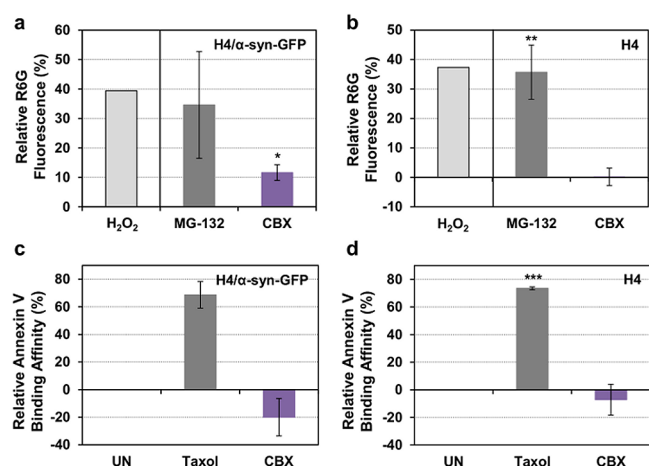

Figure 6. CBX induces the generation of intracellular ROS but does not induce apoptosis in H4 and H4/α-syn-GFP cells. (a,b) ROS generation in (a) H4/α-syn-GFP and (b) H4 cells treated with H_2O_2 (100 μM) for 1 h and MG-132 (0.5 μM) or CBX (50 μM) for 16 h was quantified by measuring rhodamine 6G fluorescence by flow cytometry (*$p < 0.05$, **$p < 0.005$). The change in fluorescence was calculated by subtracting the mean fluorescence intensity of the untreated sample from the mean fluorescence intensity of treated samples, which was normalized to the treated sample to obtain a percent value of DHR6G fluorescence. The data are reported as the mean ± SD ($n = 3$). (c,d) Relative Annexin V-binding affinity in (c) H4/α-syn-GFP and (d) H4 cells treated with taxol (50 nM) and CBX (50 μM) for 16 h (***$p < 0.01$). The data are reported as the mean ± SD ($n = 3$).

increase in R6G fluorescence. These results suggest that CBX induces mild oxidative stress, which is likely to trigger HSF1 activation and Hsp70 upregulation. We also observed a 37.4% and 35.7% increase in R6G fluorescence in H4 cells treated with H_2O_2 and MG-132, respectively, under the same conditions (Figure 6b). However, incubation of H4 cells with CBX did not result in a significant increase in R6G fluorescence, suggesting that the CBX-triggered increase in general protein aggregation in H4 cells (Figure 1b) arises from another phenomenon. Based on these data, it also cannot be excluded that additional pathways, distinct from induction of oxidative stress, may contribute to CBX-mediated activation of HSF1 and Hsp70 upregulation. These results suggest that the effect of CBX might be cell-type-specific, as previously

suggested,[26] and that CBX-mediated induction of oxidative stress is likely to have a protective effect under conditions causing proteotoxic stress such as misfolding and aggregation.

Next, we investigated whether CBX treatment under conditions that induce oxidative stress and prevent α-syn-GFP aggregation causes cytotoxicity and cell death. Apoptosis induction was evaluated in H4 and H4/α-syn-GFP cells treated with CBX (50 μM) by monitoring membrane rearrangement (Annexin V binding), which is characteristic of early apoptosis, and membrane fragmentation (propidiumiodide (PI) binding), which is characteristic of late apoptosis, as previously described.[52,53] Taxol stabilizes microtubules leading to G2/M cell cycle arrest and apoptosis[54] and was thus used as a positive control in this experiment. H4/α-syn-GFP cells treated with taxol (50 nM) presented a 68.7% increase in Annexin V binding compared to untreated cells (Figure 6c). Treatment of H4/α-syn-GFP cells with CBX did not cause cytotoxicity but resulted in a decrease (20.0%) in Annexin V binding. Similar results were obtained after incubating H4 cells with taxol and CBX under the same conditions, which resulted in a 75.3% increase and a 7.2% decrease in Annexin V binding, respectively (Figure 6d). Moreover, the small molecules tested caused no considerable changes in the relative PI-positive population in H4 and H4/α-syn-GFP cells (Supplementary Figure S6). These results indicate that CBX treatment does not cause cytotoxicity in H4/α-syn-GFP cells under conditions shown to cause mild oxidative stress and prevent α-syn-GFP aggregation.

In summary, CBX-induced HSF1 activation and Hsp70 upregulation reduces α-syn-GFP aggregation and α-syn-associated toxicity in a synucleinopathy model. Additionally, this study demonstrates, for the first time, that chemical modulation of Hsp70 activity, investigated using the Hsp70-specific modulators MAL3-101 and 115-7c, impacts α-syn aggregation, thereby validating the use of chemical modulators of Hsp70 expression and activity to reduce the accumulation of α-syn aggregates. Results from this study thus provide a proof-of-principle demonstration that chemical modulation of the Hsp70 machine is a viable therapeutic strategy for the treatment of diseases characterized by α-syn misfolding and deposition. Considering the limited penetration of CBX into the blood brain barrier,[55] these findings motivate the search for safer and more effective CBX analogues for the treatment of synucleinopathies and potentially other protein misfolding diseases caused by deposition of proteinaceous aggregates.

■ METHODS

A detailed description of the materials and methods including primers, plasmid construction, cell lines, stable transfections, aggregation studies, cell fractionation, quantitative RT-PCR, SEAP reporter assay, immunofluorescence analyses, split-GFP assay, apoptosis assay, and measurement of intracellular ROS generation is provided in the Supporting Information. Aggregation studies were conducted using the ProteoStat Aggregation detection kit (Enzo Life Sciences) according to manufacturer's protocol. Colocalization of α-syn-GFP and the ProteoStat dye in H4/α-syn-GFP cells was evaluated by fluorescence microscopy using the *Colocalization Colormap* script. ProteoStat dye fluorescence intensity was measured by flow cytometry (FACSCanto II, BD Biosciences). Additional details are provided in the Supporting Information.

1466

dx.doi.org/10.1021/cb400017h | ACS Chem. Biol. 2013, 8, 1460−1468

■ AUTHOR INFORMATION

Corresponding Author
*E-mail: segatori@rice.edu.

Notes
The authors declare no competing financial interest.

■ REFERENCES

(1) Uversky, V. N. (2008) alpha-synuclein misfolding and neuro-degenerative diseases. *Curr. Protein Pept. Sci. 9*, 507−540.

(2) Uversky, V. N. (2003) A protein-chameleon: Conformational plasticity of alpha-synuclein, a disordered protein involved in neurodegenerative disorders. *J. Biomol. Struct. Dyn. 21*, 211−234.

(3) Uversky, V. N. (2007) Neuropathology, biochemistry, and biophysics of alpha-synuclein aggregation. *J. Neurochem. 103*, 17−37.

(4) Singleton, A. B., Farrer, M., Johnson, J., Singleton, A., Hague, S., Kachergus, J., Hulihan, M., Peuralinna, T., Dutra, A., Nussbaum, R., Lincoln, S., Crawley, A., Hanson, M., Maraganore, D., Adler, C., Cookson, M. R., Muenter, M., Baptista, M., Miller, D., Blancato, J., Hardy, J., and Gwinn-Hardy, K. (2003) alpha-synuclein locus triplication causes Parkinson's disease. *Science 302*, 841−841.

(5) Zhou, W. B., Hurlbert, M. S., Schaack, J., Prasad, K. N., and Freed, C. R. (2000) Overexpression of human alpha-synuclein causes dopamine neuron death in rat primary culture and immortalized mesencephalon-derived cells. *Brain Res. 866*, 33−43.

(6) Fleming, S. M., Salcedo, J., Fernagut, P. O., Rockenstein, E., Masliah, E., Levine, M. S., and Chesselet, M. F. (2004) Early and progressive sensorimotor anomalies in mice overexpressing wild-type human alpha-synuclein. *J. Neurosci. 24*, 9434−9440.

(7) McNaught, K. S. P., Olanow, C. W., Halliwell, B., Isacson, O., and Jenner, P. (2001) Failure of the ubiquitin-proteasome system in Parkinson's disease. *Nat. Rev. Neurosci. 2*, 589−594.

(8) Muchowski, P. J. (2002) Protein misfolding, amyloid formation, and neurodegeneration: A critical role for molecular chaperones? *Neuron 35*, 9−12.

(9) Hartl, F. U., and Hayer-Hartl, M. (2002) Protein folding - Molecular chaperones in the cytosol: from nascent chain to folded protein. *Science 295*, 1852−1858.

(10) Huang, C. J., Cheng, H., Hao, S. F., Zhou, H., Zhang, X. J., Gao, J. N., Sun, Q. H., Hu, H. Y., and Wang, C. C. (2006) Heat shock protein 70 inhibits alpha-synuclein fibril formation via interactions with diverse intermediates. *J. Mol. Biol. 364*, 323−336.

(11) Luk, K. C., Mills, I. P., Trojanowski, J. Q., and Lee, V. M. Y. (2008) Interactions between Hsp70 and the hydrophobic core of alpha-synuclein inhibit fibril assembly. *Biochemistry 47*, 12614−12625.

(12) Pemberton, S., Madiona, K., Pieri, L., Kabani, M., Bousset, L., and Melki, R. (2011) Hsc70 protein interaction with soluble and fibrillar alpha-synuclein. *J. Biol. Chem. 286*, 34690−34699.

(13) Auluck, P. K., Chan, H. Y. E., Trojanowski, J. Q., Lee, V. M. Y., and Bonini, N. M. (2002) Chaperone suppression of alpha-synuclein toxicity in a Drosophila model for Parkinson's disease. *Science 295*, 865−868.

(14) Klucken, J., Shin, Y., Masliah, E., Hyman, B. T., and McLean, P. J. (2004) Hsp70 reduces alpha-synuclein aggregation and toxicity. *J. Biol. Chem. 279*, 25497−25502.

(15) Morimoto, R. I. (1998) Regulation of the heat shock transcriptional response: cross talk between a family of heat shock factors, molecular chaperones, and negative regulators. *Genes Dev. 12*, 3788−3796.

(16) Liangliang, X., Yonghui, H., Shunmei, E., Shoufang, G., Wei, Z., and Jiangying, Z. (2010) Dominant-positive HSF1 decreases alpha-synuclein level and alpha-synuclein-induced toxicity. *Mol. Biol. Rep. 37*, 1875−1881.

(17) Gestwicki, J. E., and Garza, D. (2012) Protein quality control in neurodegenerative disease. *Prog. Mol. Biol. Transl. Sci. 107*, 327−353.

(18) Holmberg, C. I., Illman, S. A., Kallio, M., Mikhailov, A., and Sistonen, L. (2000) Formation of nuclear HSF1 granules varies depending on stress stimuli. *Cell Stress Chaperones 5*, 219−228.

(19) Westerheide, S. D., Bosman, J. D., Mbadugha, B. N. A., Kawahara, T. L. A., Matsumoto, G., Kim, S. J., Gu, W. X., Devlin, J. P., Silverman, R. B., and Morimoto, R. I. (2004) Celastrols as inducers of the heat shock response and cytoprotection. *J. Biol. Chem. 279*, 56053−56060.

(20) Yamanaka, K., Takahashi, N., Ooie, T., Kaneda, K., Yoshimatsu, H., and Saikawa, T. (2003) Role of protein kinase C in geranylgeranylacetone-induced expression of heat-shock protein 72 and cardioprotection in the rat heart. *J. Mol. Cell. Cardiol. 35*, 785−794.

(21) McLean, P. J., Klucken, J., Shin, Y., and Hyman, B. T. (2004) Geldanamycin induces Hsp70 and prevents alpha-synuclein aggregation and toxicity in vitro. *Biochem. Biophys. Res. Commun. 321*, 665−669.

(22) Putcha, P., Danzer, K. M., Kranich, L. R., Scott, A., Silinski, M., Mabbett, S., Hicks, C. D., Veal, J. M., Steed, P. M., Hyman, B. T., and McLean, P. J. (2010) Brain-Permeable Small-Molecule Inhibitors of Hsp90 Prevent alpha-Synuclein Oligomer Formation and Rescue alpha-Synuclein-Induced Toxicity. *J. Pharmacol. Exp. Ther. 332*, 849−857.

(23) Pinder, R. M., Brogden, R. N., Sawyer, P. R., Speight, T. M., Spencer, R., and Avery, G. S. (1976) Carbenoxolone− Review of its pharmacological properties and therapeutic efficacy in peptic-ulcer disease. *Drugs 11*, 245−307.

(24) de Pina-Benabou, M. H., Szostak, V., Kyrozis, A., Rempe, D., Uziel, D., Urban-Maldonado, M., Benabou, S., Spray, D. C., Federoff, H. J., Stanton, P. K., and Rozental, R. (2005) Blockade of gap junctions in vivo provides neuroprotection after perinatal global ischemia. *Stroke 36*, 2232−2237.

(25) Nagayama, S., Jono, H., Suzaki, H., Sakai, K., Tsuruya, E., Yamatsu, I., Isohama, Y., Miyata, T., and Kai, H. (2001) Carbenoxolone, a new inducer of heat shock protein 70. *Life Sci. 69*, 2867−2873.

(26) Kawashima, D., Asai, M., Katagiri, K., Takeuchi, R., and Ohtsuka, K. (2009) Reinvestigation of the effect of carbenoxolone on the induction of heat shock proteins. *Cell Stress Chaperones 14*, 535−543.

(27) Sreedhar, A. S., and Csermely, P. (2004) Heat shock proteins in the regulation of apoptosis: new strategies in tumor therapy−A comprehensive review. *Pharmacol. Ther. 101*, 227−257.

(28) Salvi, M., Fiore, C., Battaglia, V., Palermo, M., Armanini, D., and Toninello, A. (2005) Carbenoxolone induces oxidative stress in liver mitochondria, which is responsible for transition pore opening. *Endocrinology 146*, 2306−2312.

(29) McLean, P. J., Kawamata, H., and Hyman, B. T. (2001) alpha-synuclein-enhanced green fluorescent protein fusion proteins form proteasome sensitive inclusions in primary neurons. *Neuroscience 104*, 901−912.

(30) Cook, N. P., Kilpatrick, K., Segatori, L., and Marti, A. A. (2012) Detection of alpha-synuclein amyloidogenic aggregates in vitro and in cells using light-switching dipyridophenazine ruthenium(II) complexes. *J. Am. Chem. Soc. 134*, 20776−20782.

(31) Shen, D., Coleman, J., Chan, E., Nicholson, T. P., Dai, L., Sheppard, P. W., and Patton, W. F. (2011) Novel cell- and tissue-based assays for detecting misfolded and aggregated protein accumulation within aggresomes and inclusion bodies. *Cell Biochem. Biophys. 60*, 173−185.

(32) Dobson, C. M. (2003) Protein folding and misfolding. *Nature* 426, 884−890.

(33) Vinken, M., Decrock, E., De Vuyst, E., Ponsaerts, R., D'Hondt, C., Bultynck, G., Ceelen, L., Vanhaecke, T., Leybaert, L., and Rogiers, V. (2011) Connexins: sensors and regulators of cell cycling. *Biochim. Biophys. Acta, Rev. Cancer* 1815, 13−25.

(34) Wang, F., Agnello, G., Sotolongo, N., and Segatori, L. (2011) Ca2+ homeostasis modulation enhances the amenability of L444P glucosylcerebrosidase to proteostasis regulation in patient-derived fibroblasts. *ACS Chem. Biol.* 6, 158−168.

(35) Zourlidou, A., Smith, M. D. P., and Latchman, D. S. (2004) HSP27 but not HSP70 has a potent protective effect against alpha-synuclein-induced cell death in mammalian neuronal cells. *J. Neurochem.* 88, 1439−1448.

(36) Fewell, S. W., Smith, C. M., Lyon, M. A., Dumitrescu, T. P., Wipf, P., Day, B. W., and Brodsky, J. L. (2004) Small molecule modulators of endogenous and co-chaperone-stimulated Hsp70 ATPase activity. *J. Biol. Chem.* 279, 51131−51140.

(37) Braunstein, M. J., Scott, S. S., Scott, C. M., Behrman, S., Walter, P., Wipf, P., Coplan, J. D., Chrico, W., Joseph, D., Brodsky, J. L., and Batuman, O. (2011) Antimyeloma effects of the heat shock protein 70 molecular chaperone inhibitor MAL3-101. *J. Oncol. 2011*, 232037.

(38) Rodina, A., Vilenchik, M., Moulick, K., Aguirre, J., Kim, J. N., Chiang, A., Litz, J., Clement, C. C., Kang, Y. L., She, Y. H., Wu, N., Felts, S., Wipf, P., Massague, J., Jiang, X. J., Brodsky, J. L., Krystal, G. W., and Chiosis, G. (2007) Selective compounds define Hsp90 as a major inhibitor of apoptosis in small-cell lung cancer. *Nat. Chem. Biol.* 3, 498−507.

(39) Patham, B., Duffy, J., Lane, A., Davis, R. C., Wipf, P., Fewell, S. W., Brodsky, J. L., and Mensa-Wilmot, K. (2009) Post-translational import of protein into the endoplasmic reticulum of a trypanosome: an in vitro system for discovery of anti-trypanosomal chemical entities. *Biochem. J.* 419, 507−517.

(40) Huryn, D. M., Brodsky, J. L., Brummond, K. M., Chambers, P. G., Eyer, B., Ireland, A. W., Kawasumi, M., LaPorte, M. G., Lloyd, K., Manteau, B., Nghiem, P., Quade, B., Seguin, S. P., and Wipf, P. (2011) Chemical methodology as a source of small-molecule checkpoint inhibitors and heat shock protein 70 (Hsp70) modulators. *Proc. Natl. Acad. Sci. U.S.A.* 108, 6757−6762.

(41) Wisen, S., and Gestwicki, J. E. (2008) Identification of small molecules that modify the protein folding activity of heat shock protein 70. *Anal. Biochem.* 374, 371−377.

(42) Wisen, S., Bertelsen, E. B., Thompson, A. D., Patury, S., Ung, P., Chang, L., Evans, C. G., Walter, G. M., Wipf, P., Carlson, H. A., Brodsky, J. L., Zuiderweg, E. R. P., and Gestwicki, J. E. (2010) Binding of a small molecule at a protein-protein interface regulates the chaperone activity of Hsp70-Hsp40. *ACS Chem. Biol.* 5, 611−622.

(43) Cabantous, S., Terwilliger, T. C., and Waldo, G. S. (2005) Protein tagging and detection with engineered self-assembling fragments of green fluorescent protein. *Nat. Biotechnol.* 23, 102−107.

(44) Kothawala, A., Kilpatrick, K., Novoa, J. A., and Segatori, L. (2012) Quantitative analysis of alpha-synuclein solubility in living cells using split GFP complementation. *PLoS One* 7, No. e43505.

(45) Jolly, C., Usson, Y., and Morimoto, R. I. (1999) Rapid and reversible relocalization of heat shock factor 1 within seconds to nuclear stress granules. *Proc. Natl. Acad. Sci. U.S.A.* 96, 6769−6774.

(46) Yokota, S., Kitahara, M., and Nagata, K. (2000) Benzylidene lactam compound, KNK437, a novel inhibitor of acquisition of thermotolerance and heat shock protein induction in human colon carcinoma cells. *Cancer Res.* 60, 2942−2948.

(47) Zundorf, G., Kahlert, S., and Reiser, G. (2007) Gap-junction blocker carbenoxolone differentially enhances NMDA-induced cell death in hippocampal neurons and astrocytes in co-culture. *J. Neurochem.* 102, 508−521.

(48) Polla, B. S., Kantengwa, S., Francois, D., Salvioli, S., Franceschi, C., Marsac, C., and Cossarizza, A. (1996) Mitochondria are selective targets for the protective effects of heat shock against oxidative injury. *Proc. Natl. Acad. Sci. U.S.A.* 93, 6458−6463.

(49) Ahn, S. G., and Thiele, D. J. (2003) Redox regulation of mammalian heat shock factor 1 is essential for Hsp gene activation and protection from stress. *Genes Dev.* 17, 516−528.

(50) Qin, Y., Lu, M., and Gong, X. (2008) Dihydrorhodamine 123 is superior to 2,7-dichlorodihydrofluorescein diacetate and dihydrorhodamine 6G in detecting intracellular hydrogen peroxide in tumor cells. *Cell Biol. Int.* 32, 224−228.

(51) Hoyt, K. R., Gallagher, A. J., Hastings, T. G., and Reynolds, I. J. (1997) Characterization of hydrogen peroxide toxicity in cultured rat forebrain neurons. *Neurochem. Res.* 22, 333−340.

(52) Wang, F., Song, W., Brancati, G., and Segatori, L. (2011) Inhibition of endoplasmic reticulum-associated degradation rescues native folding in loss of function protein misfolding diseases. *J. Biol. Chem.* 286, 43454−43464.

(53) Wang, F., Chou, A., and Segatori, L. (2011) Lacidipine remodels protein folding and Ca(2+) homeostasis in Gaucher's disease fibroblasts: A mechanism to rescue mutant glucocerebrosidase. *Chem. Biol.* 18, 766−776.

(54) Bacus, S. S., Gudkov, A. V., Lowe, M., Lyass, L., Yung, Y., Komarov, A. P., Keyomarsi, K., Yarden, Y., and Seger, R. (2001) Taxol-induced apoptosis depends on MAP kinase pathways (ERK and p38) and is independent of p53. *Oncogene* 20, 147−155.

(55) Leshchenko, Y., Likhodii, S., Yue, W., Burnham, W. M., and Velazquez, J. L. P. (2006) Carbenoxolone does not cross the blood brain barrier: an HPLC study. *BMC Neurosci.* 7, 3.